



Design, synthesis and biological evaluation of a novel class of anticancer agents: Anthracenylisoxazole lexitropsin conjugates

Xiaochun Han^b, Chun Li^b, Michael D. Mosher^{a,b}, Kevin C. Rider^{b,†}, Peiwen Zhou^{b,d}, Ronald L. Crawford^c, William Fusco^c, Andrzej Paszczynski^c, Nicholas R. Natale^{b,*,†}

^a Department of Chemistry, University of Nebraska—Kearney, Kearney, NE 68849-1150, United States

^b Department of Chemistry, University of Idaho, Moscow, ID 83844, United States

^c Environmental Biotechnology Institute, University of Idaho, Moscow, ID 83844, United States

^d AK Scientific Inc., Mountain View CA 94043, United States

ARTICLE INFO

Article history:

Received 16 October 2008

Revised 19 December 2008

Accepted 22 December 2008

Available online 31 December 2008

Keywords:

Anthracene
Anti-tumor
G-quadruplex
Isoxazole
Pyrrole

ABSTRACT

The synthesis and in vitro anti-tumor 60 cell lines screen of a novel series of anthracenyl isoxazole amides (AIMs) (While not a strict acronym, the designation AIM is in honor of the memory of Professor Albert I. Meyers.) (**22–33**) are described. The molecules consist of an isoxazole that pre-organizes a planar aromatic moiety and a simple amide and/or lexitropsin-oligopeptide. The new conjugate molecules were prepared via doubly activated amidation modification of Weinreb's amide formation technique, using SmCl_3 as an activating agent which produces improved yields for sterically hindered 3-aryl-4-isoxazole-carboxylic esters. The results of the National Cancer Institute's (NCI) 60 cell line screening assay show a distinct structure activity relationship (SAR), wherein a trend of the highest activity for molecules with one *N*-methylpyrrole peptide. Evidence consistent with a mechanism of action via the interaction of these compounds with G-quadruplex (G4) DNA and a structural based rationale for the observed selectivity of the AIMs for G4 over B-DNA is presented.

© 2009 Elsevier Ltd. All rights reserved.

1. Introduction

Small molecules that bind DNA have found application in medicine, notably as cancer chemotherapeutic agents.^{1,2} That these agents are also highly cytotoxic is attributed to their tendency to bind rather indiscriminately to DNA, and any beneficial effect arises from the more rapid death rates for faster replicating cancer cells.³ Thus, it seems a reasonable proposition that agents which are able to selectively recognize specific sequences of DNA could potentially have higher therapeutic indices.⁴ In fact, considerable effort has been devoted toward the conjugation of DNA binding pharmacophores in an attempt to recognize and selectively bind specific DNA sequences.^{5,6} The bulk of the focus of this work has, until recently, been on B-DNA.^{7–10} While this has produced a greatly increased understanding of the principles relating to the binding of small molecules to DNA, only limited progress in the development of new chemotherapeutic agents has been achieved.

The initial rationale for our work involved the use of an isoxazole to pre-organize B-DNA binding groups and thereby increase anti-

cancer efficacy.^{11,12} While our initial foray into this arena met with encouraging anti-tumor activity in screens provided by the National Cancer Institute's Developmental Therapeutics Program (NCI-DTP)^{13,14} (vide infra), we will present evidence herein that our lead molecules did not appear to exert their bioactivity by binding B-DNA. Concurrent with our studies at this time, numerous workers recognized that non-B-DNA conformations are potentially feasible targets for anti-tumor drug development. Two prominent theories recognize the G-quadruplex (G4) conformation of DNA as a potential molecular target. The first line of reasoning involves the inhibition of telomere maintenance via stabilization of the G4 conformer.^{7–10,15–18} The second theory postulates that G4 may represent an ancient off-switch for gene expression in specific oncogenes, such as *c-myc*.¹⁹ It has been argued that molecules that selectively target G4 could plausibly have unprecedented selectivity. Proof-of-concept has emerged in the form of a G4 binder which advanced to clinical trials as an anti-cancer agent.²⁰ Based on this information, we have examined systematic structural changes in our initial lead compound to test this revised hypothesis, and describe in this work the synthesis and anti-tumor activity of these compounds in the NCI-DTP 60 cell line screening protocol. The structure activity relationship (SAR) that emerges is consistent with the G4 binding working hypothesis, and is supported by evidence of G4 interaction from spectroscopy, telomerase inhibition assays, and electrospray mass spectrometry.

* Corresponding author. Tel.: +1 406 243 4132; fax: +1 406 243 5228.

E-mail address: Nicholas.natale@umontana.edu (N.R. Natale).

† NIH-COBRE Center for Structural and Functional Neuroscience, Department of Biomedical and Pharmaceutical Sciences, University of Montana, Skaggs Building 480, Missoula, MT 59812-1522, United States.

2. Chemistry

The central strategy for the preparation of the target molecules necessitated improved synthetic methodology which could overcome formidable steric encumbrance, hindrance which was required by the premise of our working hypothesis. The route to these compounds (Scheme 1) involves the initial acetylation and nitration of *N*-methylpyrrole (**1**). Amide bond formation between **3** and appropriate primary and secondary amines gave rise to the expected amidopyrroles (**6** and **12**). Reduction of the nitro group allows step-wise extension of the pyrrole chain to the desired chain length.

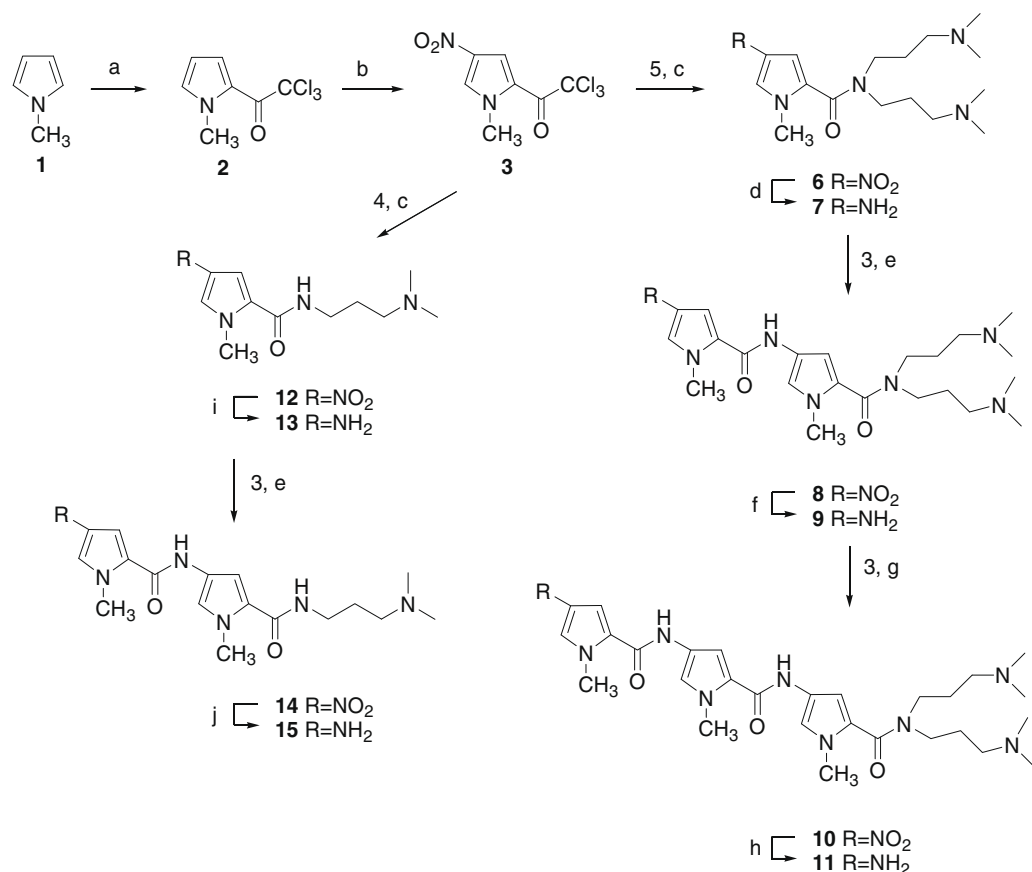
Linkage via an amide bond of the relatively unreactive heteroaromatic amines (**7**, **9**, **11**, **13**, and **15**) with rigid anthracenyl-isoxazole carboxylates was accomplished using a modification of our previously reported double activation (Scheme 2). Based on this previously developed methodology,^{21,22} we prepared a set of pyrrole-type lexitropsin oligopeptides possessing at least one moiety which would be protonated at physiological pH.

The series containing two tertiary amine groups was explored by molecular modeling studies and target molecules (**23–26**) were docked with the solid state coordinates of the G4 DNA reported by Neidle. Such studies indicated that the two ‘tails’ could plausibly increase the interaction of a lexitropsin-type molecule with the DNA phosphate backbones.

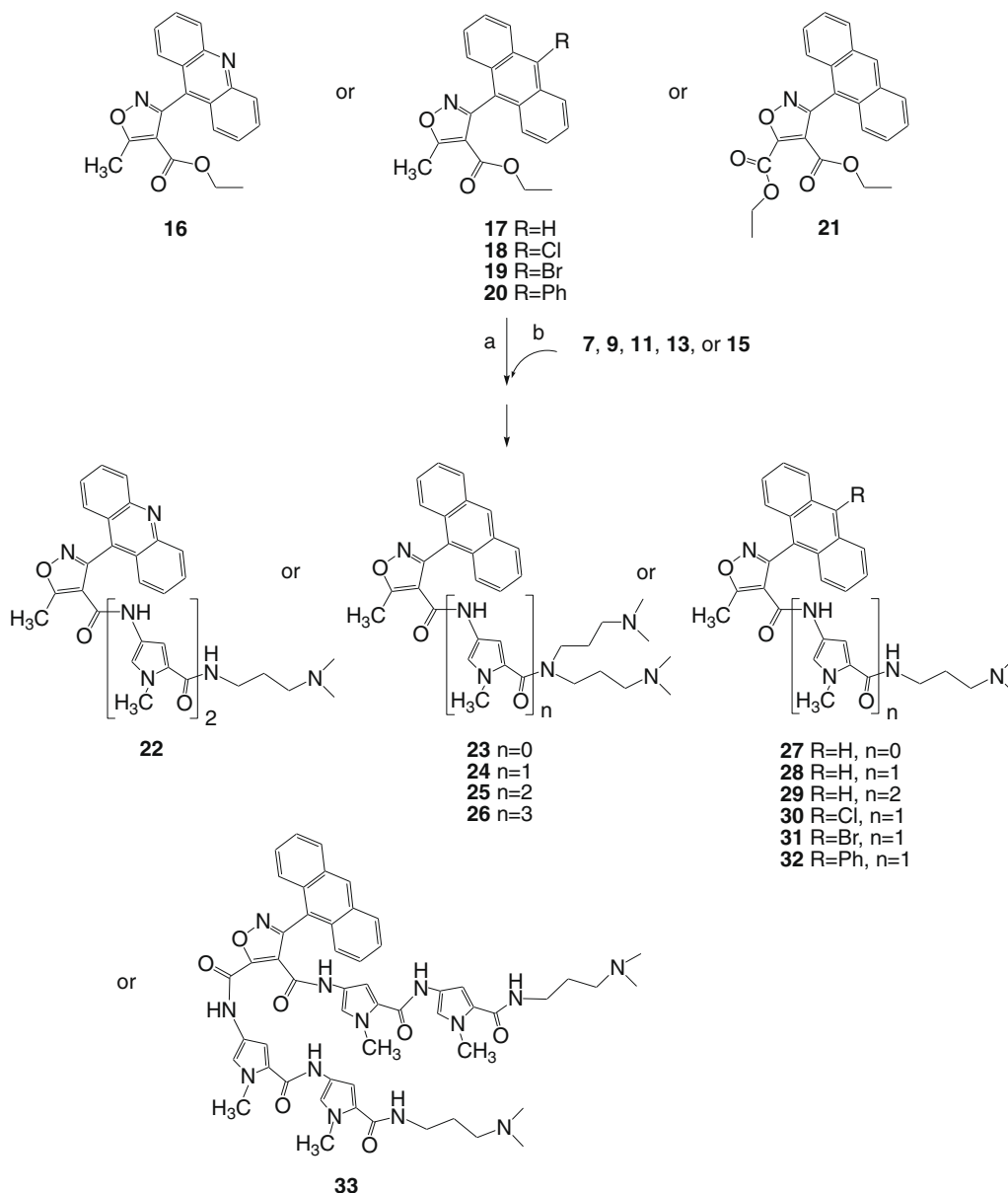
The amide formation between lexitropsin and 3-(9'-anthracenyl) 5-methyl 4-isoxazolecarboxylate **17** (prepared via the 1,3-cycloaddition of 9-anthracenyl nitrile oxide and the enamine of ethyl acetoacetate)²³ was achieved through doubly activated

amidation.¹² This amidation is actually a modification of Weinreb's amidation, which has been an effective method for direct conversion from ester to amide for many years. In the classical Weinreb's amidation,²⁴ trialkyl aluminum is mixed with free primary or secondary amine to generate dialkylaluminum amide in situ, which not only increases the nucleophilicity of the amine but also makes carboxylic ester group susceptible to attack.

Double activated amidation was applied after we tried typical Weinreb's amidation on the amide formation between an aminolexitropsin and 3-(9'-anthracenyl) 5-methyl 4-isoxazolecarboxylic ester and obtained products in only modest yield. We had previously observed by NMR that the ester group of 3-(9'-anthracenyl) 5-methyl 4-isoxazolecarboxylate is located proximal to the tricyclic aromatic system as evidenced by significant magnetic anisotropy.²³ This has also been supported by subsequent X-ray studies.²⁵ It is a reasonable expectation that the low reactivity arises from considerable steric hindrance preventing ester group interaction with the aluminum center of Weinreb's amide. In our modified methodology, the carboxylic ester was pre-mixed with a mild Lewis acid (SmCl_3) to avoid a coordinative interaction with the aluminum activated amine. In order for the Lewis acid to be compatible to the existence of basic tertiary amino group of lexitropsin as well as the utilization of alkyl aluminum, mild Lewis acid lanthanide chloride was applied. No or minimum additional coordination interaction between the lanthanide center and aluminum center is required. Two decades ago, in the study of the characteristics of lanthanide coordination catalysts for polymerization, it was suggested that SmCl_3 and EuCl_3 gave the lowest coordination interaction with alkylaluminum.²⁶ This finding indicates that



Scheme 1. Reagents and conditions: (a) trichloroacetyl chloride, ether, 0 °C to room temperature; (b) HNO_3 (fuming), acetyl anhydride, -40 °C to room temperature; (c) **5** $\text{NH}[(\text{CH}_2)_3\text{N}(\text{CH}_3)_2]_2$ or **4** $\text{NH}_2(\text{CH}_2)_3\text{N}(\text{CH}_3)_2$, THF, room temperature; (d) Pd/C, H_2 (37 psi), MeOH, room temperature; (e) **3**, THF, room temperature; (f) Pd/C, H_2 (37 psi), MeOH, room temperature; (g) **3**, THF, room temperature; (h) Pd/C, H_2 (37 psi), MeOH, room temperature; (i) Pd/C, H_2 (37 psi), MeOH, room temperature; (j) Pd/C, H_2 (37 psi), MeOH, room temperature.



Scheme 2. Reagents and conditions: (a) SmCl_3 (10%), THF, room temperature, 2 h; (b) $\text{Al}(\text{CH}_3)_3$ (1 equiv), THF, 0 °C to room temperature, 1 h; (c) THF, reflux, 36 h.

SmCl_3 or EuCl_3 may serve as ideal lanthanide Lewis acid for the doubly activated amidation.

The modified Weinreb's amidation afforded up to 80–90% yield (Scheme 2), with a variety of hindered substrates.^{27,28} This method had also been previously used to prepare the bis-lexitropsin **33**.²⁹

3. Results and discussion

Our work was initiated to find a compound that meets the needs of both DNA-intercalation and B-DNA's minor-groove binding and thus targets HIV.²³ It was reported that DNA minor groove binders (such as netropsin or distamycin analogues) linked with acridine showed greater binding affinity for DNA than either acridine or minor groove binders, and optimum linker length should consist of a chain of 5 atoms.³⁰ An isoxazole ring was then designed to tether two biologically active portions, acridine (**22**) or anthracene (**29**) and lexitropsin peptide containing polyamidopyrroles, which exhibit preference for binding to poly-AT DNA and target HIV's *tat* gene. The results from National Cancer Institute (NCI)'s

anti-HIV test showed both **22** and **29** were inactive to HIV. But surprisingly, compound **29** showed slight activity against certain human tumor cells in NCI's 60 cell line screen.^{13,14} Subsequently COMPARE^{31,32} analysis with the NCI Standard Agent Database was performed. However, it did not give a significant correlation with agents of known mechanism of action (all Pairwise Correlation Coefficients were <0.5); in contrast to the good correlations usually observed for intercalating agents.

A plethora of G-quadruplex ligands have been developed as potential molecular targets for cancer chemotherapy, such as PIPER, TMPyP, 2,6-diamidoanthraquinones, and bisamido acridines.^{15–19,33–35} Almost all of these G-quadruplex ligands have extended planar chromophores, and π - π stacking on the G-quartet end(s) is an important factor in their binding.^{19,33–36} The anthracene moiety in **29** may serve as an analogous π -electron rich planar chromophore, and provide binding to the top stack of G-quadruplex.³⁶ The lexitropsin peptide moiety was presumed to bind the TTA loop of G-quadruplex.^{4,5,37,38} This hypothesis inspired us to design a series of analogues (**23–28**, **30–32**) based on **29**.³⁹

The isoxazole moiety plays a pivotal role in our working hypothesis.⁴⁰ It is a rigid linker, pre-organizing the anthracene and peptide in three dimensions, and potentially can also function to deliver the bioconjugate molecule to the cellular DNA. Lexitropsin analogues were in different lengths, to test the hypothesis that given the binding site for 'n' pyrrole rings is 'n + 1' base pairs long in terms of contacted base pairs,^{37,38} the relationship for the $n = 0$ –3 series should be linear and increasing for B-DNA, but in contrast for G4-DNA would be expected to be maximum at $n = 1$ based on our working model (vide infra). Furthermore, introduction of an electron-pair bearing element (Cl) or group (phenyl) may provide interaction to cations in the G-quadruplex cavity, thus preferentially enhancing binding of these compounds to G4 DNA.

3.1. Testing of biological activities

3.1.1. In vitro anti-tumor activity

Structure–activity relationship (SAR) data for the anthracenyl isoxazole amides synthesized (**23**–**32**) were acquired by evaluating their in vitro anti-tumor activity against NCI's 60 human tumor cell lines.^{13,14,41,42} These cell lines have been derived from nine cancer types that adequately meet minimal quality assurance criteria representing leukemia, melanoma and cancers of the lung, colon, brain, ovary, breast, prostate, and kidney. The results are shown in Table 1. Several compounds were selected for re-screening by the Biological Evaluation Committee of NCI, and for those ranges are given (AIMs **23**, **29**, **30**, and **32**). Since single digit micromolar is a practical measure of encouraging anti-tumor activity, we use the total number of cell lines inhibited at single digit micromolar (N in Table 1) as an additional benchmark for overall activity. We also note those cell lines for which the anti-tumor efficacy was within the nanomolar regime. We started the SAR by conjugating different lengths of lexitropsin peptide derivatives (**23**–**32**), and anticipating higher anti-tumor activity as peptide length increased. Even though varying the length of peptide had a dramatic effect on anti-tumor potency, the anti-tumor activity of this series of molecules had no linear relationship with the length of lexitropsin peptide. Inside each series, either double tail (**23**–**26**) or single tail (**27**–**32**), compounds which had one pyrrole ($n = 1$) moiety gave the strongest anti-tumor activity and the broadest spectrum of inhibition at single digit micro-molar (μM) GI_{50} . Compound **24**, which had GI_{50} of 3.89 μM and inhibited 44 tumor cell lines, was 3.98 and 6.30-fold more potent than **25** and **26**, which inhibited 7 and 0 cell lines, respectively. Compound **28**, which had GI_{50} as 7.94 μM and inhibited 23 cell lines, was 4.06 and 1.32-fold more

potent than **27** and **29**, which inhibited 1 and 12 cell lines, respectively. This suggests the interaction of the conjugate molecule occurs with folded DNA structures possessing $n + 1$ (two) ATT-rich bases instead of with duplex DNA's minor groove, which requires long-chained base pair recognition structure for binding. On the other hand, compound **23**, which has no pyrrole ring in the structure, has similar GI_{50} (4.57 μM) and inhibition spectrum (42 cell lines) to that of compound **24**. Both **30** and **32** had less than 2 μM GI_{50} values, and inhibited almost all the tumor cell lines tested, indicating that introduction of electron-rich substituents at C10' of anthracene (**30** and **32**) increased anti-tumor potency.

An interesting result is that compounds **23**, **27**, **30**, and **32** showed higher activity against some colon cancer cell lines and non-small cell lung cancer cell lines, in which the *c-myc* oncogene is implicated as a potential contributing factor (Table 1).⁴³ *C-myc* expression has been reported to be downregulated by G-quadruplex stabilization.¹⁹ This suggests that compounds **23**, **27**, **30**, and **32** inhibit cells, in which *c-myc* oncogene is over expressed, by stabilizing G-quadruplex.

3.1.2. In vivo activity and acute toxicity

In light of the observation that the in vitro activity lies outside the category of adequately studied anti-tumor agents, the lead compound **29** was selected for the hollow fiber in vivo screen.⁴⁴ The total Score of 10 reflected some in vivo effect, however, the score usually required for further development is 20. The mouse toxicity assay indicated no acute toxicity for **29**, and the animals showed weight gain at day 14 for all three dose regimens (IP, single dose at day 1, as a homogeneous smooth suspension of saline plus Tween 80 at 100, 200, and 400 mg/kg). Therefore, further studies into SAR development to increase the efficacy (*op cit*) and understand the mechanism of action (vide infra) appeared warranted (Fig. 1).

3.2. Approaches toward understanding the mechanism of action (MoA)

3.2.1. Spectroscopy with oligonucleotides

An oligonucleotide microarray experiment was conducted wherein the effect of **29** on Calf thymus DNA and an oligonucleotide designed by Hurley, (5'-CATGGTGGTTT(GGGTTA)₄CCAC-3') known to form a quadruplex in solutions of KCl and NaCl,⁴⁵ was examined. The microarray fluorescence experiment for the mixture of Calf Thymus (CT) DNA with **29** indicates a quenching of the fluorescence but shows no bathochromic shift which would be consis-

Table 1
Synopsis of in vitro anti-tumor activities of compounds (**22**–**33**) against the NCI-DTP 60 cell line screen

AIM compound	–Log (mean GI_{50}) ^a	Mean GI_{50} (μM)	N^b	Efficacy ^c
16	4.69	20.4	2	
22	4.68	20.9	0	
23	5.31–5.34	4.90–4.57	37–42	Non-small cell lung cancer EKVX: 6.18, colon cancer HCC-2998: 6.11, CNS cancer SF-295: 7.52
24	5.41	3.89	44	
25	4.81	15.5	7	
26	4.61	24.5	0	
27	4.49	32.4	1	Non-small cell lung cancer NCI-H226: <8.00
28	5.10	7.94	23	Non-small cell lung cancer HOP-62: 6.39
29	4.91–4.98	12.3–10.5	12–14	
30	5.72–5.75	1.91–1.78	53–57	Non-small cell lung cancer HOP-92: 7.03
31	5.06	8.71	18	CNS cancer SNB-75: 6.80
32	5.71–6.04	1.95–0.91	60	CNS cancer SF-539: <8.00, Non-small cell lung cancer HOP-62: 7.98, HOP-92: 7.2
33	4.69	20.4	2	

The full 60 cell line data is available free of charge on the internet at the NCI-DTP site [<http://dtp.nci.nih.gov/index.html>]. NSC numbers are provided for each compound in this table in the Supplementary data.

^a Range given for those compounds selected for a second screening by NCI's Biological Evaluation Committee.

^b The number of cell lines inhibited at single digit micromolar.

^c Cell lines inhibited in the nanomolar range, with –Log GI_{50} .

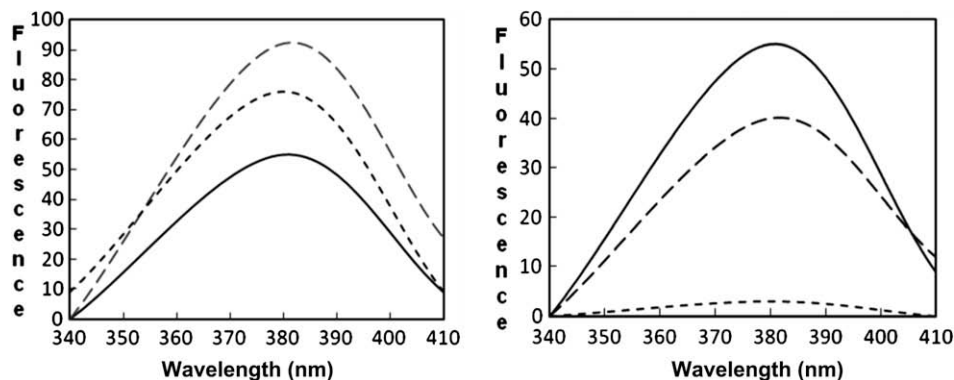


Figure 1. Fluorescence spectra of oligonucleotide microarray experiment. Left: Normalized Fluorescence spectra of AIM-29 alone (solid line), CT-DNA alone (long-dashed line) and the Hurley Oligonucleotide alone (small-dashed line). Right: Normalized Fluorescence spectra of AIM-29 alone (solid line), with CT-DNA (long-dashed line) and the Hurley-sequence Oligonucleotide (small-dashed line).

tent with an anthracene intercalation mechanism (Fig. 2).^{46,47} The Hurley-Oligonucleotide experiment with **29** shows considerable quenching of the fluorescence which is consistent with a π -stacking interaction with the G-tetrad of the quadruplex structure that forms in situ under the experimental conditions.^{48,49}

The oligonucleotide and CT-DNA solutions were prepared in a 10 mM KCl solution containing a TE buffer at pH = 7.0 with a final concentration of 400 $\mu\text{g}/\mu\text{L}$. The oligonucleotide solution was hybridized using a cyanine dye (Cy3-AP3-dCTP) utilizing a 96-well plate. AIM-2 was in an aqueous 25% DMSO solution (10 μM). All experiments were carried out at 37 °C with oligonucleotide solutions being incubated for 5 min prior to printing on the slide for analysis. All spectra were taken at four excitation wavelengths (310 nm, 380 nm, 410 nm, and 485 nm) with 530 nm emission. All microarray experiments were run on a GenePix 4000 microarray fluorescence scanner with 10 μm resolution and a dynamic detection range of four orders of magnitude which is linear over three orders of magnitude.

An additional fluorescence experiment involving **29** with human DNA (1:1 M ratio), *sans* the histones, was performed (data not shown). The results of the second fluorescence experiment

were an 11 nm hypsochromic shift in the λ_{max} which is inconsistent with an intercalative mechanism⁴⁷ and is likely due to hydrogen bonding interactions and/or solvation of **29** in the presence of the DNA. Further fluorescence-DNA-titration experiments are warranted in light of these results.

3.2.2. COMPARE analysis^{31,32,50,51}

We used **29** as a probe or seed compound in the NCI's COMPARE Algorithm to rank the similarity of responses of the 60 cell lines to the standard agent database.^{13,14,41,42} Similarity of pattern to that of the seed is expressed quantitatively as a Pearson correlation coefficient (PCC). The results obtained with the COMPARE algorithm indicate that compounds high in this ranking may possess a mechanism of action (MoA) similar to that of the seed compound.^{31,32} COMPARE works quite well for intercalating/topoisomerase II inhibitors. The top ten matches for adriamycin, with a PCC range of 0.758–0.950, were all topoisomerase II inhibitors. In contrast, **29**—originally thought by our group to be a potential intercalating/minor groove binder—indicted no strong correlation to any consistent MoA, with the highest PCC being a relatively weak 0.517 (Table 2). Similar COMPARE analysis of **23–26**

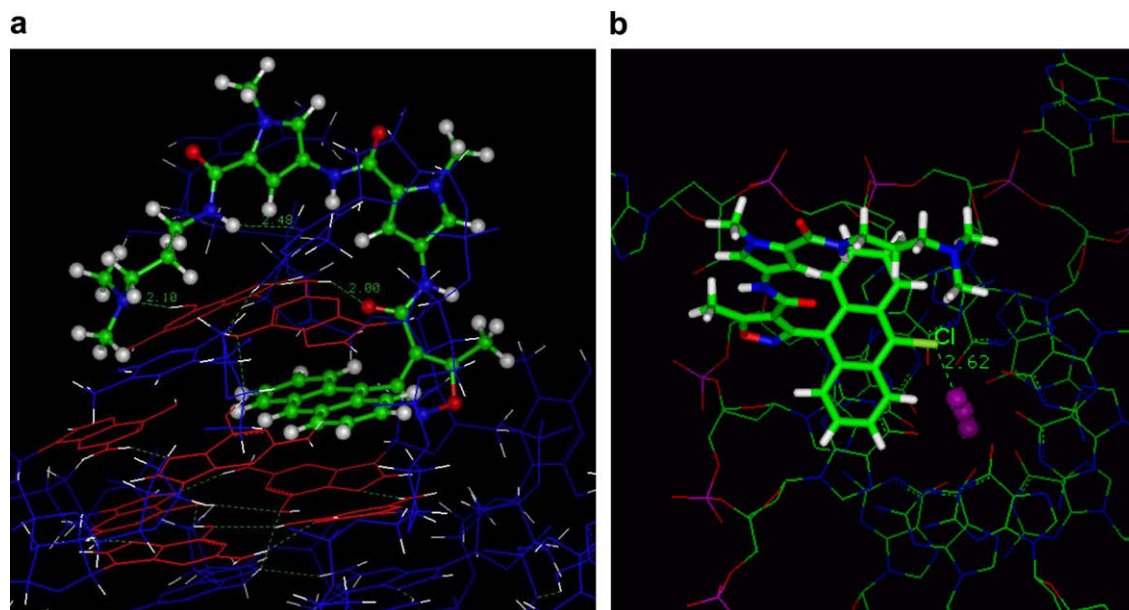


Figure 2. Plausible Docking modes of compounds **29** and **30**. (a) Left, the Intercalative mode, where **29** is shown displacing a guanine after minimization. (b) Right, the stacking mode with ligand **30**, after minimization the chlorine nestles within a reasonable association distance with the potassium in the G-tetrad.

indicated no significant correlation with any MoA in the Standard Agent Data Base.

3.2.3. Computation

The dihedral angle between the tricyclic planar aromatic moiety and the isoxazole from our crystallographic studies of intermediates and analogs, is in the range of 74–80°. The idealized helical pitch angle for B-DNA was estimated to be ca. 47.1° by Goodsell and Dickerson in their isohelical analysis of groove-binding drugs.^{54,55} Therefore, we calculated the energy associated with conformational changes to this dihedral angle in order to determine whether B-DNA binding seemed plausible. The rotational barrier calculations were performed using the torsion force constraint in the Discover module.⁵⁶ The bond in question was rotated through 360 intervals (1° increments) using a force constant of 10. After each rotation, the structure was subjected to 1000 steps of minimization, or until an rms value of 0.01 was reached, using the VA09A algorithm. The results of the conformational searches were examined with the Analysis module by constructing a table of total energy verses dihedral angle. Calculations from the INSIGHT II program suggests that this energetic cost is high, precisely in the vicinity of the helical pitch angle requisite for binding of a C-3 aromatic isoxazole to B-DNA (Table 3).

In combination with the COMPARE analysis, we felt it was prudent to consider alternatives to B-DNA as a molecular target.

3.2.4. Revision of the working hypothesis

In light of the increasingly numerous reports postulating G4 binding as a mechanism for anti-tumor activity, and given an overall similarity of some of the salient structural features of our compounds, we conducted a number of computational studies with the G4 coordinates available from Neidle's elegant crystallographic studies.^{57,58}

In a typical example, the minimum energy structure of NSCD 694332 and quadruplex DNA⁵⁷ was calculated in a SGI INSIGHT 2000 docking study, using the cvff forcefield, and all the solution molecules (H₂O) were removed. The DNA molecule was constrained and the distance between first potassium and C-10 hydrogen was initially set to 4.00 Å. After 3000 iterations using steepest descent minimization, in most cases the drug-receptor interaction had converged to a final energy, which the program reported as consisting of separate electrostatic and VdW components. If the minimization did not reach convergence at a set number of iterations, reasonable and slight adjustments were made to the ligand structure, and minimization was repeated until a convergent structure solution was obtained.²⁷

Two of the possible docking modes we considered are illustrated in Figure 2. In the first we initiated the docking with the anthracenyl moiety intercalated between the G-tetrads. During minimization, the anthracene of **29** displaced two of the guanines (in red). In the minimized structure (Fig. 2a), the isoxazole ring N is

Table 2
COMPARE analysis using **29**, NSC D-694332, as 'seed'

Anti-tumor agent	PCC	Mechanism
Tetrandrine	0.517	Calcium channel blocker
Macbecin II	0.488	DNA anti-metabolite
Didemnin B	0.468	Inhibits ribosomal protein synthesis
Tetrocarcin A	0.462	Modulates mitochondrial apoptosis
Spirogermanium	0.459	Alkylating agent
Pibenzimol	0.453	Minor groove binder
Thalicarpine	0.450	Unknown
Neocarzinostatin	0.436	Enediyne strand breaker
Fostriecin	0.421	Topo II catalytic inhibitor
Emofolin sodium	0.415	DHFR inhibitor
Vinblastin sulfate	0.414	Antimitotic agent

Table 3
Energy calculation of rotation toward isoxazole/anthracene coplanarity

Angle (°)	Energy (kcal)
Energy difference from 90°	
120.14	6.96
121.44	7.87
122.24	8.82
123.44	10.46
124.24	11.73
125.44	13.96
126.24	15.70
127.44	18.76
128.24	21.16
129.34	25.03
130.54	30.19
131.34	35.08
132.54	42.40
133.44	48.40
134.24	65.10
135.44	68.00

within 3 Å of the NH₂ of the guanine of the lower, intact G-tetrad. Alternatively, we considered an external stacking (Fig. 2b), and in the case of analog **30** which contained a group bearing lone pairs at C(10) of the anthracenyl group, C(10) tended to orient—again after minimization—within 2.62 Å over the potassium in the cavity of the G-tetrad.

Similar features which emerged from both of these minimized structures were (1) the isoxazole nitrogen was within hydrogen bonding distance of the guanine 2-amino group of the G-tetrad, and (2) the amine of the dimethylamino tail would move slightly to associate proximal to a group peripheral to the intact G-tetrad, as seen in the case of **30**, with the phosphate in the sugar-phosphate TTA loop.

Thus, there is a specific structure-based reason for the expectation that the AIMs should be selective for G4 DNA at the expense of B. The energy cost of B-DNA binding is increased by the mismatch with the helical pitch angle.

3.2.5. Telomeric repeat amplification protocol (TRAP) assay

Stabilizing G-quadruplex inhibits telomerase activity, and this has been correlated with inhibition of cancer growth.⁵⁹ Thus, until recently the TRAP assay has been widely used to assess G-quadruplex interaction. We reported in 2004 that the fluorescence analysis TRAP assay was marred by the inhibition of *taq* polymerase by **32**,⁶⁰ and this recently has been verified by Mergny's group.⁶¹ In the more reliable gel electrophoresis TRAP analysis, AIM **30** did indeed appear to inhibit telomere elongation rather than *taq* polymerase (data for both TRAPese and TRAP is shown in the Supplementary data), however, we sought a more direct method of determining G4 interaction with our compounds, and therefore also examined electrospray mass spectrometry (vide infra).

3.2.6. Electrospray ionization mass spectrometry (ESI-MS) study of G-quadruplex DNA stabilization by **30** or **32**⁶²

Total ions of G-quadruplex DNA, i-motif DNA, and duplex DNA were measured under the same conditions (Fig. 3). In the absence of G4 stabilizing ligands (negative control), ion intensities of single-stranded DNA dropped dramatically, while duplex formation is rather fast. Rehybridization in the absence of G4 stabilizing ligands proceeded to 50% completion in 10 min and was essentially complete in 45 min (negative control, shown in Supplementary data).

When incubated with either TMPy4 (positive control), **30** or **32**, the decrease of single-stranded DNA signals and increase of duplex signals were dramatically slowed. Although no DNA-ligand complex ion was detected, the inhibition of duplex formation

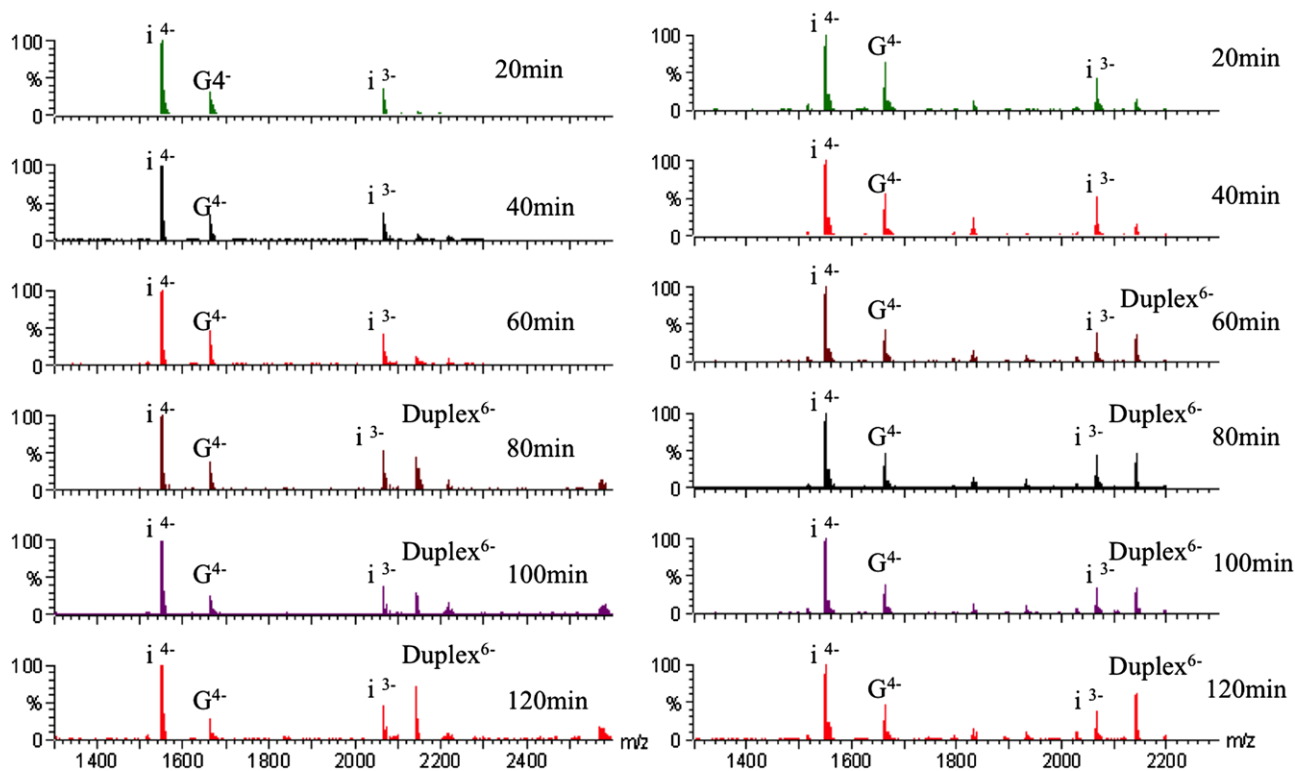


Figure 3. ESI-MS spectra comparison between **32** and TMPyP4. Left: ESI-MS spectra of a mixture of 5 μM G-DNA, 5 μM **32**, and 5 μM C-DNA at different time. Right: ESI-MS spectra of a mixture of 5 μM G-DNA, 5 μM TMPyP4, and 5 μM C-DNA at the times indicated.

indicated interference from both TMPyP, **30**, and **32** in DNA annealing, which suggests the ability for G-quadruplex stabilization. The slopes of ion intensity trend lines give approximate inhibition abilities of TMPyP4 and **32**. For example, slopes in total duplex ion intensity trends showed that TMPyP4 inhibited duplex formation at a comparable rate to **32**, where both took about 80 min to proceed to 50% hybridization, and significant ions corresponding to single stranded oligonucleotides were still present even at 2 h.

4. Conclusion

The new compounds reported in this study showed *in vitro* anti-tumor activity, and the mean GI_{50} against the NCI60 cell line panel for the length of the oligopyrrole moiety ($n =$ the number of pyrroles) was observed as $1 > 0 \gg 2 > 3$ for the bis-dimethylaminopropyl series **23–26** and $1 > 2 \gg 0$ for the mono-dimethylaminopropyl series **(27–29)**; and for the anthracenyl C(10) position was $\text{Ph} \approx \text{Cl} \gg \text{H} > \text{Br}$ (**28, 30–32**), with the most efficacious examples having average activity comparable to agents currently in general medical practice.¹³ The activity correlates *inversely* with the length of lexitropsin oligopeptides within the conjugate molecules, that is, conjugates containing a *single pyrrole ring* demonstrated the strongest activity and broadest spectrum of inhibition against cancer cell lines. The SAR, spectroscopic and ESI-MS assays are consistent with our current working hypothesis that the compounds selectively target G4 sequences. In conclusion, the results presented suggest that the synthesis of a new series of anthracenyl isoxazole-lexitropsin conjugates, the AIMs, may represent a potential useful addition to the arsenal of anti-cancer molecules. In addition, we present structure-based evidence for the contention that the AIMs are unique among G4 binding agents in that they possess specific features which destabilize their intercalative interaction with B-DNA, and therefore, the expectation of selectivity is reasonable. Further clarification of

the MoA and the effects of substitution at C5 of the isoxazole, and on the anthracene appears warranted. Those results will be reported in due course.

5. Experimental

Mass spectra were obtained on a JEOL JMS-AX505 HA. The NMR spectra (^1H and ^{13}C) were obtained on a Bruker AVANCE 300 and 500 Digital NMR (300 and 500 MHz, respectively) using SGI-IRIX 6.5. Elemental analysis was performed by Desert Analytics Laboratory, PO BOX 41838, Tucson, AZ 85717. All reactions were performed under an inert atmosphere of nitrogen or argon. Tetrahydrofuran was distilled from sodium-benzophenone immediately before use. Flash chromatography was performed on silica gel (Merck 60 Å, 230–400 mesh) with freshly distilled solvents. Pyrrole starting materials **2** and **3** were prepared according to Nishwaki.²² 3-(9'-Anthracenyl) 5-methyl 4-isoxazolecarboxylate **17**, and the corresponding acridine **16**,²³ anthracenyl ring analogs **18–20**^{27,28} and final product **33**²⁹ were prepared according to methodology previously reported by our lab.

5.1. 2-[[[N,N-Bis[3-(N,N-dimethylamino)propyl]amino]carbonyl]-1-methyl-4-nitropyrrole (**6**)]

To a solution of **3** (9.24 g, 35.88 mmol) in THF (40 mL), was added a solution of 3,3'-iminobis(*N,N*-dimethylpropylamine) (25.24 g, 134.74 mmol) at room temperature. The reaction mixture was heated at reflux for 3 h. The reaction mixture was cooled to room temperature and the solvent was evaporated. The residue was then purified by chromatography on silica gel eluting with MeOH/triethylamine (9/1) ($R_f = 0.40$) to give yellow oil **6** (4.82 g, 41.3%), which became a pale yellow solid after being triturated with hexane (20 mL); mp: 60–61 °C; ^1H NMR (CDCl_3): δ 7.69 (1H, d, $J = 1.7$ Hz), 7.66 (1H, d, $J = 1.7$ Hz), 3.96 (3H, s), 3.67 (4H, t,

$J = 7.5$ Hz), 2.43–2.35 (16H, m), 1.94 (4H, m). ^{13}C NMR (CDCl_3): δ 162.4, 135.4, 127.2, 125.5, 106.7, 57.0, 46.0, 45.7, 37.0, 26.2. MS (CI): m/z (%) 340 ($M+1$, 100), 268 (8.62), 268 (8.62), 84 (12.83), 58 (18.52). Anal. Calcd for $\text{C}_{16}\text{H}_{29}\text{N}_5\text{O}_3$: C, 56.62; H, 8.61; N, 20.63. Found: C, 56.64; H, 8.33; N, 20.09.

5.2. 2-[[[2-[[[*N,N*-bis[3-(*N,N*-dimethylamino)propyl]amino]carbonyl]-1-methyl-1*H*-pyrrol-4-yl]amino]carbonyl]-1-methyl-3-nitropyrrole (8)

To a solution of **6** (2.40 g, 7.38 mmol) in MeOH (175 mL), was added Pd/C (5%) (2.50 g). The mixture was hydrogenated at 37–40 psi at room temperature for 3 h. The catalyst was removed by filtration and the solvent was removed in vacuo. To a solution of the above residue in THF (40 mL), was added a solution of **3** (3.05 g, 11.73 mmol) within 10 min. The reaction mixture was stirred at room temperature for 3 h. Solvent was removed in vacuo and the residue was then purified by chromatography on silica gel eluting with MeOH/triethylamine (9/1) ($R_f = 0.34$) to give pale yellow solid, 2.21 g (65%); mp: 125–127 °C. ^1H NMR (CDCl_3): δ 9.12 (1H, s), 7.61 (1H, d, $J = 1.8$ Hz), 7.47 (1H, d, $J = 1.8$ Hz), 7.25 (1H, d, $J = 1.8$ Hz), 6.36 (1H, d, $J = 1.8$ Hz), 4.07 (3H, s), 3.71 (3H, s), 3.54 (4H, t, $J = 7.8$ Hz), 2.34 (4H, t, $J = 7.2$ Hz), 2.28 (12H, s), 1.85 (4H, m). ^{13}C NMR (CDCl_3): δ 164.1, 157.8, 135.2, 127.1, 126.8, 123.9, 121.3, 117.0, 107.8, 103.6, 57.1, 45.8, 45.6, 38.4, 36.1, 27.0; MS (CI): m/z (%) 462 ($M+1$, 100), 377 (19.91), 352 (14.52), 170 (67.70), 84 (28.51), 58 (17.97).

To a solution of **8** (100 mg, 0.2 mmol) in absolute ethanol (5 mL), was added a solution of oxalic acid dihydrate ($\text{C}_2\text{O}_4\text{H}_2 \cdot 2\text{H}_2\text{O}$) (57 mg, 0.45 mmol). The mixture was stirred at room temperature until no more precipitate formed. The solid was filtered and washed with absolute ethanol (5 mL \times 5). The oxalic acid salt of **8** was obtained after being dried in vacuo to yield a solid (109 mg, 90%), mp: 203–204 °C. Anal. Calcd for $\text{C}_{22}\text{H}_{35}\text{N}_7\text{O}_4 \cdot 1.5\text{C}_2\text{O}_4\text{H}_2 \cdot 0.5\text{H}_2\text{O}$: C, 49.58; H, 6.49; N, 16.19. Found: C, 49.81; H, 6.64; N, 16.05.

5.3. 2-[[[2-[[[2-[[*N,N*-bis[3-(*N,N*-dimethylamino)propyl]amino]carbonyl]-1-methyl-1*H*-pyrrol-4-yl]amino]carbonyl]-1-methyl-1*H*-pyrrol-4-yl]amino]carbonyl]-1-methyl-4-nitropyrrole (10)

To a solution of **8** (1.13 g, 2.45 mmol) in MeOH (90 mL), was added Pd/C (5%) (2.00 g). The mixture was hydrogenated at 37–40 psi at room temperature for 3 h. The catalyst was removed by filtration and the solvent was removed in vacuo. To a solution of the above residue in THF (30 mL), was added a solution of **3** (1.00 g, 3.90 mmol) within 10 min. The reaction mixture was stirred at room temperature for 3 h. Solvent was removed in vacuo and the residue was then purified by chromatography on silica gel eluting with MeOH/triethylamine (9/1) ($R_f = 0.21$) to give pale yellow solid, (0.74 g, 52%); mp: 178–179 °C; ^1H NMR ($\text{DMSO}-d_6$): δ 10.29 (1H, s), 9.89 (1H, s), 8.18 (1H, d, $J = 1.7$ Hz), 7.58 (1H, d, $J = 1.7$ Hz), 7.24 (2H, d, $J = 1.7$ Hz), 7.03 (1H, d, $J = 1.7$ Hz), 6.37 (1H, d, $J = 1.7$ Hz); 3.96 (3H, s), 3.85 (3H, s), 3.58 (3H, s), 2.49 (4H, t, $J = 7.7$ Hz), 2.15 (4H, t, $J = 7.1$ Hz), 2.10 (12H, s), 1.70–1.61 (4H, m). ^{13}C NMR (CDCl_3): δ 164.6, 159.2, 158.1, 135.4, 127.3, 126.7, 124.0, 123.6, 123.0, 121.8, 120.0, 117.6, 108.5, 102.9, 102.6, 57.1, 46.4, 45.6, 38.7, 37.2, 35.9, 27.1. MS (CI): m/z (%) 584 ($M+1$, 55.96), 397 (10.47), 275 (24.39), 153 (18.31), 149 (52.19), 122 (32.51), 107 (20.18), 101 (16.14), 81 (100). Anal. Calcd for $\text{C}_{28}\text{H}_{41}\text{N}_9\text{O}_5$: C, 57.62; H, 7.08; N, 21.60. Found: C, 57.23; H, 7.26; N, 21.24.

5.4. Ethyl 3-(10'-phenyl-9'-anthracenyl)-5-methyl-4-isoxazole-carboxylate (20)

A mixture of ethyl 3-(10'-bromo-9'-anthracenyl)-5-methyl-4-isoxazolecarboxylate (420 mg, 1.02 mmol), phenyl boronic acid

(140 mg, 1.15 mmol), $\text{Pd}_2(\text{dba})_3$ (45 mg, 5 mol %), $\text{P}(\text{t-Bu})_3$ (10% in hexane, 242 mg, 12 mol %) and KF (191 mg, 3.3 mmol) in THF (7 mL) was stirred at room temperature under argon atmosphere for 72 h. The reaction mixture was filtered and the solid was washed by THF (10 mL). The filtrate was concentrated and purified by chromatography on silica gel eluting with hexane/benzene (3:2) to give yellow crystal (382 mg, 92%); mp: 178–180 °C. ^1H NMR (CDCl_3): δ 7.62 (4H, m), 7.52 (3H, m), 7.32 (6H, m), 3.68 (2H, q, $J = 7.2$ Hz), 2.88 (3H, s), 0.33 (3H, t, $J = 7.2$ Hz). ^{13}C NMR (CDCl_3): δ 176.2, 161.5, 160.8, 139.3, 138.6, 131.2, 131.1, 130.5, 129.7, 129.0, 128.5, 128.4, 128.3, 127.6, 127.1, 125.9, 125.5, 125.1, 122.8, 111.5, 60.1, 13.5, 12.8. MS (EI): m/z (%) 407 (M^+ , 100), 319 (17.91), 295 (12.85), 252 (13.86). Anal. Calcd for $\text{C}_{27}\text{H}_{21}\text{NO}_3$: C, 79.59; H, 5.19; N, 3.44. Found: C, 79.94; H, 5.09; N, 3.57.

5.5. 3-(9-Anthracenyl)-*N,N*-bis[3-(*N,N*-dimethylamino)propyl]-5-methyl-4-isoxazolecarboxamide (23)

To a suspension of anhydrous SmCl_3 (0.21 g, 0.79 mmol) in THF (6 mL) was added ethyl 3-(9-anthracenyl)-5-methyl-4-isoxazole-carboxylate **17** (0.25 g, 0.72 mmol) in dry THF (5 mL). The slurry was stirred under nitrogen at room temperature for 5.5 h and was used in the following step.

To a solution of 3,3'-iminobis(*N,N*-dimethylpropylamine) (0.222 g, 1.19 mmol) in THF (10 mL) was added $(\text{CH}_3)_3\text{Al}$ (2 M in hexane, 0.75 mL) at 0 °C during 30 min. The resulting yellow solution was warmed to room temperature, and stirred for an additional 1 h.

The yellow-brown solution of the activated amino-lexitropsin solution was transferred via cannula to the activated ester slurry, at room temperature during 10 min. The mixture was then heated to reflux for 8 h, after which time $\text{Na}_2\text{SO}_4 \cdot 10\text{H}_2\text{O}$ (1.0 g) and cold methanol (20 mL) were added to the reaction mixture in order to quench the excessive $(\text{CH}_3)_3\text{Al}$. Solid was removed via centrifugation and a red solution was separated. The red solution was then concentrated and purified by chromatography on silica gel (200–400 mesh) eluting with methanol–30% NH_4OH (95:5), to afford **23** as a yellow oil (0.32 g, 87%). ^1H NMR (CDCl_3): δ 8.58 (1H, s), 8.06–8.00 (4H, m), 7.54–7.47 (4H, m), 3.06 (2H, t, $J = 7.1$ Hz), 2.74 (3H, s), 2.53 (2H, t, $J = 7.1$ Hz), 2.00 (6H, s), 1.87 (6H, s), 1.63 (2H, t, $J = 6.9$ Hz), 1.45 (2H, t, $J = 6.9$ Hz), 1.11–0.95 (2H, m), 0.90–0.83 (2H, m). ^{13}C NMR (CDCl_3): δ 170.8, 163.1, 157.8, 131.4, 131.1, 130.8, 130.3, 129.7, 129.3, 128.8, 128.7, 128.3, 127.1, 126.2, 125.8, 125.3, 121.9, 116.3, 56.2, 47.4, 46.4, 45.6, 45.4, 42.5, 26.7, 24.9, 11.5; MS (CI): m/z (%) 473 ($M+1$, 100), 188 (22.58), 58 (18.63).

To a solution of **23** (94 mg, 0.2 mmol) in absolute ethanol (5 mL), was added a solution of oxalic acid dihydrate ($\text{C}_2\text{O}_4\text{H}_2 \cdot 2\text{H}_2\text{O}$) (57 mg, 0.45 mmol). The mixture was stirred at room temperature until no more precipitate formed. The solid was filtered and washed with absolute ethanol (5 mL \times 5). The oxalic acid salt of **23** was obtained after being dried in vacuo to yield a solid (114 mg, 84%), mp: 185–186 °C. Anal. Calcd for $\text{C}_{29}\text{H}_{36}\text{N}_4\text{O}_2 \cdot 2\text{-C}_2\text{H}_2\text{O}_4 \cdot 1.5\text{H}_2\text{O}$: C, 58.31; H, 6.38; N, 8.24. Found: C, 58.50; H, 6.12; N, 8.12.

5.6. 3-(9-Anthracenyl)-*N*-[2-[[*N,N*-bis[3-(*N,N*-dimethylamino)propyl]amino]carbonyl]-1-methyl-1*H*-pyrrol-4-yl]-5-methyl-4-isoxazolecarboxamide (24)

To a suspension of anhydrous SmCl_3 (0.21 g, 0.79 mmol) in THF (10 mL) was added **17** (0.25 g, 0.72 mmol) in dry THF (10 mL). The slurry was stirred under nitrogen at room temperature for 5.5 h and was used in the following step.

A suspension of 10% Pd/C (0.2 g) in a solution of **6** (0.385 g, 1.19 mmol) in methanol (30 mL), was stirred for 4.5 h under H_2 pressure (37 psi) at room temperature. The catalyst was removed

by filtration, and the solvents removed in vacuo. The hydrogenation product was dissolved into dry THF (15 mL) and $(\text{CH}_3)_3\text{Al}$ (2 M in hexane, 0.75 mL) was added at 0 °C during 30 min. The mixture turned brown. The reaction was warmed to room temperature, and stirred for an additional 1 h.

By the same double activation procedure described for **23**, after the reaction work-up and separation, **24** was obtained as a pale yellow solid (0.396 g 84%), mp: 109–111 °C. ^1H NMR (CDCl_3): δ 8.63 (1H, s), 8.04 (2H, dd, $J = 0.9, 8.3$ Hz), 7.65 (2H, dd, $J = 0.9, 8.3$ Hz), 7.52–7.23 (4H, m), 6.56 (1H, d, $J = 1.7$ Hz), 6.40 (1H, s), 4.90 (1H, d, $J = 1.7$ Hz), 3.37 (3H, s), 3.21 (4H, t, $J = 6.6$ Hz), 2.94 (3H, s), 2.24–1.90 (16H, m), 1.60–1.45 (4H, m), 1.52 (2H, s). ^{13}C NMR (CDCl_3): δ 176.3, 163.9, 158.0, 157.9, 157.8, 157.6, 131.5, 131.2, 130.7, 129.2, 128.9, 128.4, 128.2, 127.9, 126.5, 125.8, 125.7, 125.3, 124.3, 120.7, 120.3, 116.1, 113.2, 57.2, 46.4, 45.8, 35.6, 26.6, 14.0. MS (CI): m/z (%) 595 (M+1, 100), 510 (6.09), 336 (19.88). Anal. Calcd for $\text{C}_{35}\text{H}_{42}\text{N}_6\text{O}_3 \cdot \text{H}_2\text{O}$: C, 68.60; H, 7.24; N, 13.71. Found: C, 68.33; H, 6.94; N, 13.61.

5.7. 3-(9-Anthracenyl)-N-[2-[[[2-[[N,N-bis[3-(N,N-dimethylamino)propyl]amino]carbonyl]-1-methyl-1H-pyrrol-4-yl]amino]carbonyl]-1-methyl-1H-pyrrol-4-yl]-5-methyl-4-isoxazolecarboxamide (25)

By the same procedure as that described for **24**, from SmCl_3 (0.21 g, 0.79 mmol), **17** (0.25 g, 0.72 mmol), 10% Pd/C (0.2 g), **8** (0.55 g, 1.19 mmol) and $(\text{CH}_3)_3\text{Al}$ (2 M in hexane, 0.75 mL), **25** was obtained as a pale yellow solid (0.44 g 78%); mp: 118–120 °C (dec). ^1H NMR (CDCl_3): δ 8.72 (1H, s), 8.12 (2H, dd, $J = 0.9, 8.2$ Hz), 7.70 (2H, dd, $J = 0.9, 8.2$ Hz), 7.55–7.50 (4H, m), 7.19 (1H, s), 7.09 (1H, d, $J = 1.7$ Hz), 6.41 (1H, s), 6.28 (1H, d, $J = 1.7$ Hz), 6.10 (1H, d, $J = 1.7$ Hz), 5.69 (1H, d, $J = 1.7$ Hz), 3.65 (3H, s), 3.61 (3H, s), 3.48 (4H, t, $J = 7.8$ Hz), 2.99 (3H, s), 2.28–2.10 (16H, m), 1.83–1.69 (4H, m), 1.52 (5H, s). ^{13}C NMR (CDCl_3): δ 176.7, 164.3, 158.7, 158.5, 157.8, 131.5, 131.3, 130.9, 129.3, 129.0, 128.6, 128.4, 128.0, 126.6, 125.9, 125.7, 125.3, 124.3, 123.6, 121.2, 120.6, 120.5, 118.8, 116.7, 113.0, 103.3, 103.2, 103.0, 57.3, 46.4, 45.7, 36.9, 35.9, 26.8, 14.1. MS (FAB): m/z (%) 717 (M+1, 71), 530, (13.19), 286 (15.85), 230 (12.43), 271 (12.37), 244 (59.35), 214 (20.21), 188 (12.72), 149 (61.28), 122 (49.88), 106 (16.22), 81 (100). Anal. Calcd for $\text{C}_{41}\text{H}_{48}\text{N}_8\text{O}_4 \cdot 2.5\text{H}_2\text{O}$: C, 64.63; H, 7.01; N, 14.71. Found: C, 64.77; H, 6.64; N, 15.08.

5.8. 3-(9-Anthracenyl)-N-[2-[[[2-[[[2-[[N,N-bis[3-(N,N-dimethylamino)propyl]amino]carbonyl]-1-methyl-1H-pyrrol-4-yl]amino]carbonyl]-1-methyl-1H-pyrrol-4-yl]amino]carbonyl]-1-methyl-1H-pyrrol-4-yl]-5-methyl-4-isoxazolecarboxamide (26)

By the same procedure as that described for **24**, from SmCl_3 (0.21 g, 0.79 mmol), **17** (0.25 g, 0.72 mmol), 10% Pd/C (0.2 g), **10** (0.693 g, 1.19 mmol) and $(\text{CH}_3)_3\text{Al}$ (2 M in hexane, 0.75 mL), **26** was obtained as a pale yellow solid (0.37 g, 56%), mp: 131–133 °C (dec). ^1H NMR (CDCl_3): δ 8.56 (1H, s), 7.96 (2H, dd, $J = 0.8, 8.1$ Hz), 7.62 (2H, dd, $J = 0.8, 8.1$ Hz), 7.46–7.30 (4H, m), 7.08 (1H, d, $J = 1.8$ Hz), 6.98 (1H, s), 6.89 (1H, d, $J = 1.8$ Hz), 6.59 (1H, s), 6.38 (1H, d, $J = 1.8$ Hz), 6.28 (1H, d, $J = 1.8$ Hz), 6.23 (1H, d, $J = 1.8$ Hz), 6.20 (1H, d, $J = 1.8$ Hz), 5.78 (1H, s), 3.83 (3H, s), 3.58 (3H, s), 3.54 (3H, s), 3.44 (4H, t, $J = 7.2$ Hz), 2.91 (3H, s), 2.16–2.10 (16H, m), 1.72–1.65 (4H, m), 1.53 (3H, s). ^{13}C NMR (CDCl_3): δ 179.6, 176.6, 176.0, 175.6, 170.8, 169.8, 159.6, 159.3, 158.5, 158.0, 131.4, 130.7, 129.1, 128.2, 128.1, 127.7, 126.3, 125.5, 124.9, 123.7, 123.5, 122.2, 121.9, 120.5, 120.1, 119.4, 118.9, 117.01133, 104.3, 103.9, 103.4, 57.0, 46.1, 45.4, 36.8, 36.7, 35.6, 13.8. MS (FAB): m/z (%) 839 (M+1, 43), 717 (11.64), 286 (29.71), 277 (15.81), 271 (25.40), 244 (100), 214 (31.05), 149 (87.91), 123 (64.75), 85 (86.34). Anal. Calcd for $\text{C}_{47}\text{H}_{54}\text{N}_{10}\text{O}_5 \cdot 1.5\text{H}_2\text{O}$: C, 65.18; H, 6.63; N, 16.17. Found: C, 65.37; H, 6.56; N, 15.83.

5.9. 3-(10'-Chloro-9'-anthracenyl)-N-[2-[[N-[3-(N,N-dimethylamino)propyl]amino]carbonyl]-1-methylpyrrol-4-yl]-5-methyl-4-isoxazolecarboxamide (30)

By the same procedure as that described for **24**, except for refluxing for 18 h, from SmCl_3 (393.5 g, 1.53 mmol), **18** (381.3 mg, 1.04 mmol), 10% Pd-C (310.6 mg), **12** (473.0 g, 1.86 mmol) and $(\text{CH}_3)_3\text{Al}$ (2 M in hexane, 2 mL), **30** was obtained as a pale yellow solid (203.7 mg, 36%), mp: 208–210 °C. ^1H NMR (CDCl_3): δ 8.65 (2H, dt, $J = 5.4, 0.6$ Hz), 7.78 (1H, br), 7.73 (2H, dt, $J = 5.4, 0.6$ Hz), 7.69 (2H, m), 7.57 (2H, m), 6.76 (1H, d, $J = 1.2$ Hz), 6.40 (1H, s), 5.19 (1H, d, $J = 1.2$ Hz), 3.72 (3H, s), 3.31 (2H, q, $J = 3.6$ Hz), 3.02 (3H, s), 2.36 (2H, t, $J = 3.6$ Hz), 2.08 (3H, s), 1.58 (2H, m). ^{13}C NMR (CDCl_3): δ 176.5, 161.1, 157.7, 157.0, 132.8, 131.3, 128.5, 128.1, 127.6, 125.5, 125.4, 123.8, 120.2, 119.8, 118.3, 112.9, 101.5, 59.4, 45.4, 39.9, 36.5, 25.1, 13.8. MS (CI): m/z (%) 544.00 (M^+ , 65.88), 306.90 (58.70), 288.92 (24.86), 153.96 (100), 136.99 (90.87). Anal. Calcd for $\text{C}_{30}\text{H}_{30}\text{ClN}_5\text{O}_3$: C, 66.23; H, 5.56; N, 12.87. Found: C, 66.07; H, 5.50; N, 12.71.

5.10. 3-(10'-Br-9'-anthracenyl)-N-[2-[[N-[3-(N,N-dimethylamino)propyl]amino]carbonyl]-1-methylpyrrol-4-yl]-5-methyl-4-isoxazolecarboxamide (31)

By the same procedure as that described for **30**, from SmCl_3 (481.5 mg, 1.87 mmol), **19** (341.6 mg, 0.83 mmol), 10% Pd/C (490 mg), **12** (458.5 mg, 1.80 mmol) and $(\text{CH}_3)_3\text{Al}$ (2 M in hexane, 2 mL), **31** was obtained as a yellow solid (280 mg, 61%), mp: 201.5–203.5 °C. ^1H NMR (CDCl_3): δ 8.70 (2H, d, $J = 9$ Hz), 7.71 (5H, m), 7.60 (2H, m), 7.57 (2H, m), 6.74 (1H, d, $J = 1.5$ Hz), 6.40 (1H, s, br), 5.24 (1H, d, $J = 1.5$ Hz), 3.74 (3H, s), 3.32 (2H, q, $J = 3.6$ Hz), 3.04 (3H, s), 2.38 (2H, t, $J = 3.6$ Hz), 2.11 (6H, s), 1.61 (2H, m). ^{13}C NMR (CDCl_3): δ 176.4, 161.0, 157.7, 157.0, 131.4, 130.3, 128.4, 128.0, 127.9, 127.0, 125.4, 123.8, 121.3, 119.7, 118.2, 112.9, 101.6, 59.3, 45.4, 39.7, 36.4, 25.2, 13.6. MS (CI): m/z (%) 590.01 (M+1, 100.00), 588.02 (99.87), 542.97 (19.06), 485.88 (22.84), 321.85 (31.82), 242.96 (20.71), 153.99 (50.75), 136.00 (51.68), 129.09 (65.34), 84.38 (43.93). Anal. Calcd for $\text{C}_{30}\text{H}_{30}\text{BrN}_5\text{O}_3$: C, 61.23; H, 5.14; N, 11.90. Found: C, 61.16; H, 5.29; N, 11.62.

5.11. 3-(10'-Phenyl-9'-anthracenyl)-N-[2-[[N-[3-(N,N-dimethylamino)propyl]amino]carbonyl]-1-methylpyrrol-4-yl]-5-methyl-4-isoxazolecarboxamide (32)

By the same procedure as that described for **30**, from SmCl_3 (491.5 mg, 1.90 mmol), **19** (300.6 mg, 0.73 mmol), 10% Pd/C (553 mg), **12** (500.5 mg, 1.97 mmol) and $(\text{CH}_3)_3\text{Al}$ (2 M in hexane, 2 mL), **32** was obtained as a pale yellow solid, 130 mg (30%), mp: 126–128 °C. ^1H NMR (CDCl_3): δ 7.68 (3H, m), 7.45 (10H, m), 6.49 (1H, s), 6.47 (1H, s), 5.37 (1H, s), 3.65 (3H, s), 3.25 (2H, q, 3.6 Hz), 2.96 (3H, s), 2.27 (2H, t, $J = 3.6$ Hz), 2.01 (6H, s), 1.53 (2H, m). ^{13}C NMR (CDCl_3): δ 176.2, 161.5, 160.1, 157.3, 139.4, 138.8, 131.4, 131.1, 130.5, 129.7, 129.0, 128.5, 128.4, 128.3, 127.6, 127.1, 125.9, 125.5, 125.1, 123.8, 122.8, 119.8, 118.1, 111.5, 101.7, 60.1, 45.4, 39.6, 36.1, 25.0, 13.4. MS (EI): m/z (%) 587 (M+1, 39.04), 586 (M^+ , 100), 585 (M-1, 19.26), 484 (13.13), 320 (19.84). Anal. Calcd for $\text{C}_{36}\text{H}_{35}\text{N}_5\text{O}_3$: C, 73.82; H, 6.02; N, 11.96. Found: C, 68.39; H, 5.85; N, 11.60.

5.12. In vitro anti-tumor assays

The NCI's in vitro anti-tumor screen (Alley, Scudiero, et al., 1988; Boyd, 1989; Boyd and Paull, 1995)^{13,50,51} consists of 60 human tumor cell lines against which compounds **22–33** are tested at a minimum of five concentrations at 10-fold dilutions. A 48 h

continuous drug exposure protocol is used, and a sulforhodamine B (SRB) protein assay is used to estimate cell viability or growth.

Acknowledgments

N.R.N. thanks the National Institute of Neurological Disease and Stroke for Grant NS38444 and P2ORR015583. We would like to thank the University of Idaho Research Council, and the National Cancer Institute for financial support. Dr. Dan Zaharevitz assisted us with the COMPARE calculation and interpretation. X.H., C.L. and K.C.R. acknowledge the Malcolm and Carol Renfrew Scholarship Endowment, University of Idaho. C.L. and K.C.R. also thank P2ORR16454.

Supplementary data

Supplementary data associated with this article can be found, in the online version, at doi:10.1016/j.bmc.2008.12.056.

References and notes

- Hurley, L. H. *J. Med. Chem.* **1989**, *32*, 2027.
- Damia, G.; Broggin, M. *Eur. J. Cancer* **2004**, *40*, 2550.
- Di Marco, A. *Antibiot. Chemother.* **1978**, *23*, 216.
- Dervan, P. B. *Science* **1986**, *232*, 464.
- Dervan, P. B. *Bioorg. Med. Chem.* **2001**, *9*, 2215.
- Bailly, C.; Chaires, J. B. *Bioconjugate Chem.* **1998**, *9*, 513.
- Cech, T. R. *Nature* **1988**, *332*, 777.
- Zahler, A. M.; Williamson, J. R.; Cech, T. R.; Prescott, D. M. *Nature* **1991**, *350*, 718.
- Cech, T. R. *Angew. Chem.* **2000**, *39*, 34.
- Phan, A. T.; Mergny, J.-L. *Nucleic Acids Res.* **2002**, *30*, 4618.
- Verner, E. J.; Oliver, B. J.; Schlicksupp, L.; Natale, N. R. *Heterocycles* **1990**, *31*, 327.
- Zhou, P.; Mosher, M. D.; Taylor, W. D.; Crawford, G. A.; Natale, N. R. *Bioorg. Med. Chem. Lett.* **1997**, *7*, 2455.
- Boyd, M. R. *Principles Pract. Oncol.* **1989**, *3*, 1.
- Sausville, E. A.; Johnson, J. I.; Cragg, G. M.; Decker, S. Cancer Drug Discovery and Development: New Paradigms for a New Millennium. In *Anticancer Agents, Frontiers in Cancer Chemotherapy*; Ojima, I., Vite, G. D., Altmann, K., Eds.; ACS Symposium Series 796; ACS: Washington, DC, 2001; p 1.
- Han, H.; Hurley, L. H. *Trends Pharmacol. Sci.* **2000**, *21*, 136.
- Hurley, L. H.; Wheelhouse, R. T.; Sun, D.; Kerwin, S. M.; Salazar, M.; Ferdoroff, O. Y.; Han, F. X.; Han, H.; Zbicka, E.; Von Hoff, D. D. *Pharmacol. Ther.* **2000**, *85*, 141.
- Neidle, S. *Chem. Br.* **2000**, *36*, 27.
- Neidle, S.; Kelland, L. R. *Anti-Cancer Drug Des.* **1999**, *14*, 341.
- Siddiqui-Jain, A.; Grand, C. L.; Bearss, D. J.; Hurley, L. H. *Proc. Natl. Acad. Sci. U.S.A.* **2002**, *99*, 11593.
- Mehta, A. K.; Shayo, Y.; Vankayalapati, H.; Hurley, L. H.; Schaefer, J. *Biochemistry* **2004**, *43*, 11953.
- Gendler, P. L.; Rapoport, H. *J. Med. Chem.* **1981**, *24*, 33.
- Nishiwaki, E.; Tanaka, S.; Lee, H.; Shibuya, M. *Heterocycles* **1988**, *27*, 1945.
- Mosher, M. D.; Natale, N. R. *J. Heterocycl. Chem.* **1995**, *32*, 779.
- Basha, A.; Lipton, M.; Weinreb, S. M. *Tetrahedron Lett.* **1977**, 4171.
- Mosher, M. D.; Natale, N. R.; Vij, A. *Acta Crystallogr., Sect. C* **1996**, *C52*, 2513.
- Shen, Z. Q.; Wang, F. S.; Hu, Z. Y.; Yu, F. S.; Qian, B. G. *J. Polym. Sci., Polym. Chem. Ed.* **1980**, *18*, 3345.
- Han, X.; Li, C.; Rider, K. C.; Blumenfeld, A.; Twamley, B.; Natale, N. R. *Tetrahedron Lett.* **2002**, *43*, 7673.
- Han, X.; Twamley, B.; Natale, N. R. *J. Heterocycl. Chem.* **2003**, *40*, 539.
- Han, X.; Natale, N. R. *J. Heterocycl. Chem.* **2001**, *38*, 415.
- Eliadis, A.; Phillips, D. R.; Reiss, J. A.; Skorobogaty, A. *J. Chem. Soc., Chem. Commun.* **1988**, 1049.
- Bai, R. L.; Paull, K. D.; Herald, C. L.; Malspeis, L.; Pettit, G. R.; Hamel, E. *J. Biol. Chem.* **1991**, *266*, 15882.
- Paull, K. D.; Lin, C. M.; Malspeis, L.; Hamel, E. *Cancer Res.* **1992**, *52*, 3892.
- Mergny, J. L.; Helene, C. *Nature Med.* **1998**, *4*, 1366.
- Mergny, J. L.; Mailliet, P.; Lavelle, F.; Riou, J. F.; Laoui, A. *Anti-Cancer Drug Des.* **1999**, *14*, 327.
- Kerwin, S. M. *Curr. Pharm. Des.* **2000**, *6*, 441.
- Cuesta, J.; Read, M. A.; Neidle, S. *Mini-Rev. Med. Chem.* **2003**, *3*, 11.
- Youngquist, R. S.; Dervan, P. B. *Proc. Natl. Acad. Sci. U.S.A.* **1985**, *82*, 2565.
- White, S.; Baird, E. E.; Dervan, P. B. *Chem. Biol.* **1997**, *4*, 569.
- Arola, A.; Vilar, R. *Curr. Top. Med. Chem.* **2008**, *8*, 1405.
- Wakefield, B. J.; Wright, D. J. *Adv. Heterocycl. Chem.* **1979**, *25*, 147.
- Alley, M. C.; Scudiero, D. A.; Monks, A.; Hursey, M. L.; Czerwinski, M. *J. Cancer Res.* **1988**, *48*, 589.
- Boyd, M. R.; Paull, K. D. *Drug Dev. Res.* **1995**, *34*, 91.
- (a) Mitani, S.; Kamata, H.; Fujiwara, M.; Aoki, N.; Tango, T.; Fukuchi, K.; Oka, T. *Clin. Exp. Med.* **2001**, *1*, 105; (b) Broers, Jos L. V.; Viallet, Jean; Jensen, Sandra M.; Harvey, Pass; Travis, William D.; Minna, John D.; Linnoila, R. Ilona. *Am. J. Res. Cell Mol. Biol.* **1993**, *9*, 33; (c) Arango, D.; Mariadason, J. M.; Wilson, A. J.; Yang, W.; Corner, G. A.; Nicholas, C.; Aranes, M. J.; Augenlicht, L. H. *Br. J. Cancer* **2003**, *89*, 1757; (d) Simonsson, T.; Pecinka, P.; Kubista, M. *Nucleic Acids Res.* **1998**, *26*, 1167.
- (a) Hollingshead, M. G.; Alley, M. C.; Camalier, R. F.; Abbott, B. J.; Mayo, J. G.; Malspeis, L.; Grever, M. R. *Life Sci.* **1995**, *57*, 131; (b) Bollini, M.; Casal, J. J.; Bruno, A. M. *Bioorg. Med. Chem.* **2008**, *16*, 8003.
- Han, F. X.; Wheelhouse, R. T.; Hurley, L. H. *J. Am. Chem. Soc.* **1999**, *121*, 3561.
- Wozczk, M.; Grzesiak, E.; Kowalczyk, D.; Ostaszewski, R. *Proc. SPIE* **2002**, *4749*, 259.
- Kumar, C. V.; Asuncion, E. H. *J. Am. Chem. Soc.* **1993**, *115*, 8541.
- Samudrala, R.; Zhang, X.; Wadkins, R. M.; Mattern, D. L. *Bioorg. Med. Chem.* **2007**, *15*, 186.
- Zhuang, X.; Tang, J.; Hao, Y.; Tan, Z. *J. Mol. Recognit.* **2007**, *20*, 386.
- http://dtp.nci.nih.gov/docs/compare/compare_intro.html. Last accessed on Nov. 25, 2008.
- Boyd, M. R.; Paull, K. D.; Rubinstein, L. R. In *Cytotoxic Anticancer Drugs: Models and Concepts for Drug Discovery and Development*; Vliorote, F. A., Corbett, T. H., Baker, L. H., Eds.; Kluwer Academic: Hingham, MA, 1992; p 11.
- Li, C.; Twamley, B.; Natale, N. R. *Acta Crystallogr., Sect. E* **2006**, *E62*, o854.
- Li, C.; Twamley, B.; Natale, N. R. *J. Heterocycl. Chem.* **2008**, *45*, 259.
- Goodsell, D.; Dickerson, R. E. *J. Med. Chem.* **1986**, *29*, 727.
- Goodsell, D. S.; Ng, H. L.; Kopka, M. L.; Lown, J. W.; Dickerson, R. E. *Biochemistry* **1995**, *34*, 16654.
- Zamponi, G.; Stotz, S. C.; Staples, R. J.; Rogers, T. A.; Nelson, J. K.; Hulubei, V.; Blumenfeld, A.; Natale, N. R. *J. Med. Chem.* **2003**, *46*, 87.
- Parkinson, G. N.; Lee, M. P.; Neidle, S. *Nature* **2002**, *417*, 876.
- Clark, G. R.; Pytel, P. D.; Squire, C. J.; Neidle, S. *J. Am. Chem. Soc.* **2003**, *125*, 4066.
- (a) Kim, N. M.; Piatyszek, M. A.; Prowse, K. R.; Harley, C. B.; West, M. D.; Ho, P. L. C.; Coviello, G. M.; Wright, W. E.; Weinrich, S. L.; Shay, J. W. *Science* **1994**, *266*, 2011; (b) Gomez, D.; Mergny, J.-L.; Riou, J.-F. *Cancer Res.* **2002**, *62*, 3365.
- Li, C.; Rider, K.; Fusco, W.; Natale, N. R.; Crawford, R. Synthesis and Activity of Anti-cancer Compounds that Target G-quadruplex DNA, 227th ACS National Meeting, Anaheim, CA, March 28–April 1, 2004. MEDI 142. See also, *Chemical & Engineering News*, March 8, 2004, p. TECH-76.
- DeCian, A.; Cristofari, G.; Reichenbach, P.; De Lemos, E.; Monchaud, D.; Teulade-Fichou, M.; Shin-ya, K.; Lacroix, L.; Lingner, J.; Megny, J. *PNAS* **2007**, *104*, 17347.
- (a) Rosu, F.; Gabelica, V.; Houssier, C.; Colson, P.; Pauw, E. D. *Rapid Commun. Mass Spectrom.* **2002**, *16*, 1729; (b) Rosu, F.; Gabelica, V.; Shin-ya, K.; De Pauw, E. *Chem. Commun.* **2003**, 2702.